

RESEARCH ARTICLE

[View Article Online](#)
[View Journal](#) | [View Issue](#)



Cite this: *Org. Chem. Front.*, 2024, **11**, 1395

Received 11th November 2023,
Accepted 6th January 2024
DOI: 10.1039/d3qo01866k
rsc.li/frontiers-organic

Iodine radical mediated cascade [3 + 2] carbocyclization of ene-vinylidenecyclopropanes with thiols and selenols *via* photoredox catalysis†

Zhe Meng,^a Min Shi ^{*a,b} and Yin Wei ^{*b}

An iodine radical mediated cascade [3 + 2] carbocyclization of ene-vinylidenecyclopropanes with thiols and selenols *via* photoredox catalysis has been reported in this paper. With this visible light-induced photocatalytic protocol, an efficient synthetic methodology for the rapid construction of sulfur- and selenium-containing polycyclic derivatives in moderate to good yields has been realized with broad substrate scope. Mechanistic investigations were also performed using control experiments, deuterium labeling and Stern–Volmer analysis as well as DFT calculations, suggesting that this cascade cyclization reaction stems from an iodine radical addition to the allenyl moiety of ene-vinylidenecyclopropane along with a cascade cyclization. Then, the reaction proceeds through a cyclopropane-ring opening pathway along with a HAT process and an intramolecular substitution. Further transformation of the obtained product has also been disclosed.

Introduction

Sulfur-containing polycyclic compounds play a significant bioactive role in natural products, pharmaceuticals and polymeric materials.¹ Moreover, in the field of life sciences, disulfide bonds can enhance the stability of polypeptides and realize biological functions of proteins.^{1c} For example, gliocladine C is a fungal metabolite that possesses a unique molecular structure and potent activities against parasites, viruses, bacteria and cancer cells (Scheme 1a).² With regard to selenium, which is in the same main group as sulfur, selenium-containing compounds generally exhibit more potent biological activity than their sulfur-containing counterparts.³ In addition, a prominent feature of selenium compounds is the fact that they are more easily absorbed by cancer cells, although the mechanism of selective selenium uptake in cancer cells is still not completely understood.⁴ For instance, β -lapachone-selenide can exert submicromolar inhibitory activity toward tumor cells but weak

cytotoxic activity toward normal cells (Scheme 1a).^{3d} Considering the above factors, the design and synthesis of chalcogen-containing polycyclic compounds have attracted great interest in recent years.⁵

The synthesis of complex polycyclic molecules has always been a momentous research subject in synthetic chemistry, especially for the preparation of multiple cyclic systems within one step.⁶ As an eco-friendly and cost-effective accelerator, iodine and its derivatives present undisputed advantages in most cases, including being easily operated and metal-free, as well as affording economies of resource, time, and labor. It is well known that the coordination between the electrophilic iodine cation and the unsaturated bond can generate the corresponding iodonium ion,⁷ which would be subsequently attacked by other unsaturated groups within the molecule, triggering a cascade cyclization reaction to obtain the iodocyclization products (Scheme 1b).⁷ For example, our group reported a novel cascade process for the synthesis of 3,3'-diphenyl-1,1'-spirobi[indene] derivatives from propargyl alcohol-tethered alkylidenecyclopropanes in the presence of I_2 .^{7e} In addition, Liang's group presented iodine promoted cascade cycloisomerization of 1-en-6,11-diyynes for the easy preparation of tetrahydrobenzo[f]isoquinolines.^{7j} On the other hand, recently with the rapid development of visible light-induced photocatalysis in organic synthesis, iodine and its derivatives have been widely utilized in a variety of photo-induced transformations.⁸ It has been known that I^- can be oxidized by photosensitizers through a SET process to form the iodine radical; moreover, I_2 can also undergo a homolytic cleavage reaction through photo-

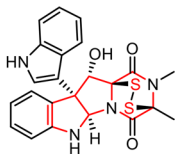
^aKey Laboratory for Advanced Materials and Institute of Fine Chemicals, School of Chemistry & Molecular Engineering, East China University of Science and Technology, 130 Meilong Road, Shanghai 200237, China

^bState Key Laboratory of Organometallic Chemistry, Center for Excellence in Molecular Synthesis, Shanghai Institute of Organic Chemistry, University of Chinese Academy of Sciences, Chinese Academy of Sciences, 345 Lingling Road, Shanghai 200032, China. E-mail: mshi@mail.sioc.ac.cn, weiyin@sioc.ac.cn

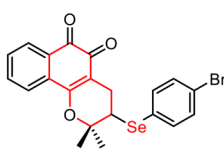
† Electronic supplementary information (ESI) available: Experimental procedures and characterization data of new compounds. CCDC 2073868 and 2244043. For ESI and crystallographic data in CIF or other electronic format see DOI: <https://doi.org/10.1039/d3qo01866k>



a) Examples of chalcogen-containing polycyclic bioactive compounds and pharmaceutical molecules

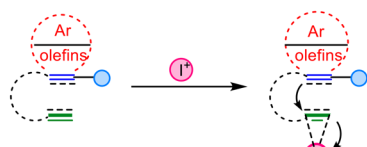


(+)-Gliocladin C
Activities against viruses etc.

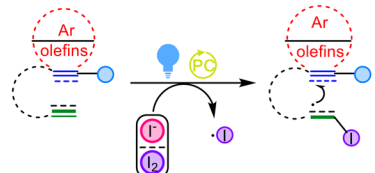


β -Lapachone-selenide
Inhibitory tumor cell activity

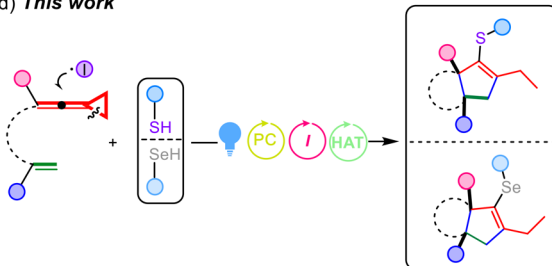
b) Cascade cyclization induced via iodine cations (iodine)



c) Cascade cyclization induced via iodine radicals



d) This work



Scheme 1 Chalcogen-containing cyclic compounds, previous work and this work.

excitation to give the iodine radical.^{8g–8i} Thus, the *in situ* generated iodine radical tends to be subsequently captured by unsaturated groups, leading to an intramolecular cascade cyclization reaction (Scheme 1c).

We previously investigated a series of cyclization reactions of ene-vinylidene cyclopropanes (ene-VDCPs)⁹ with radical-based reagents under different conditions, providing a variety of nitrogen-containing heterocycles.^{9e} In view of the aforementioned research circumstances, we wish to report in this paper a novel iodine radical mediated cascade [3 + 2] carbocyclization of ene-vinylidene cyclopropanes *via* photoredox catalysis upon visible light irradiation, delivering sulfur- or selenium-containing polycyclic derivatives under mild conditions (Scheme 1d).

Results and discussion

We first utilized substrate **1a** as the model substrate for the initial investigation and subsequently optimized the reaction

Table 1 Optimization of the reaction conditions^a

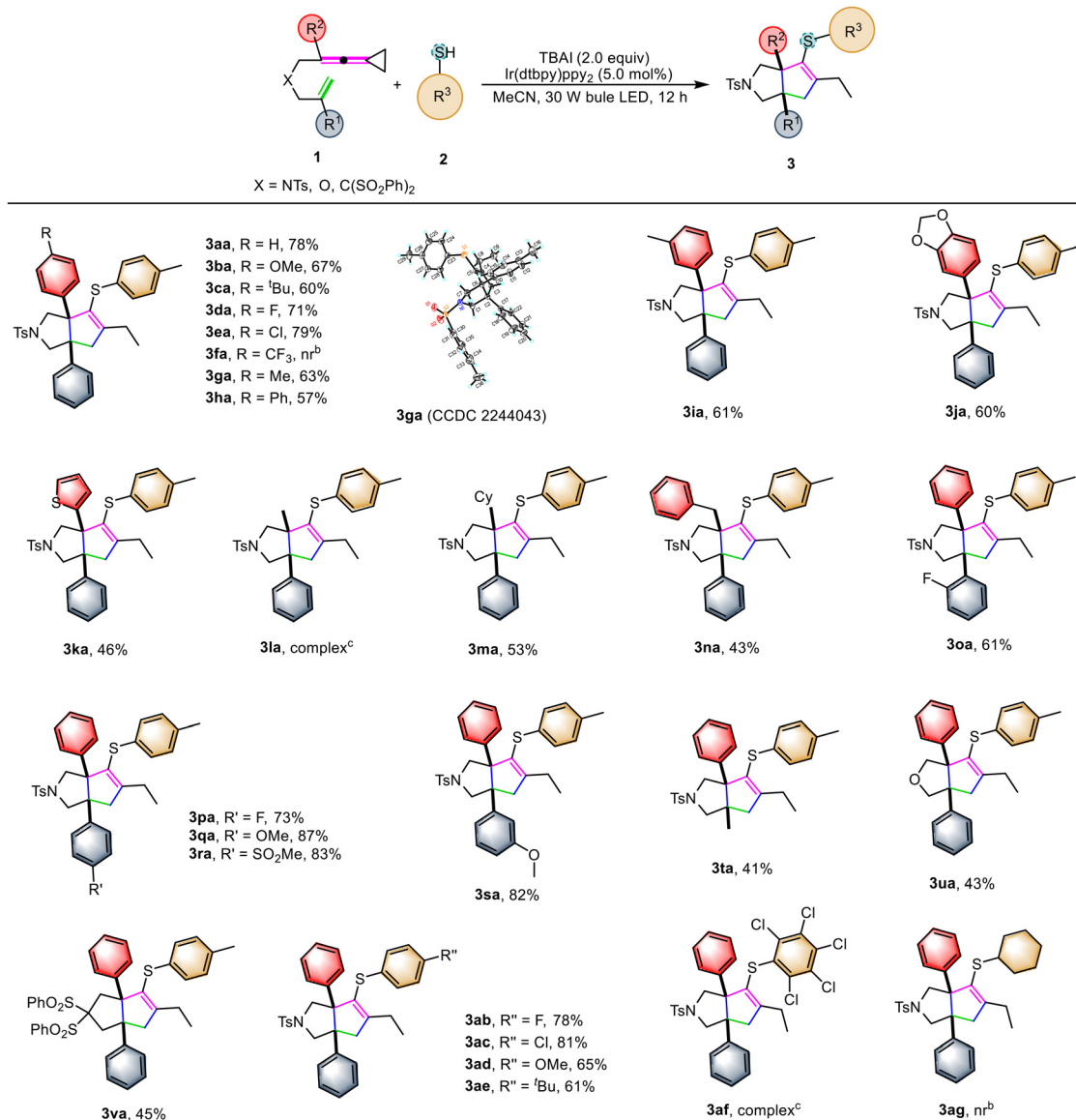
Entry ^a	Variation from the standard conditions	3aa , Yield ^b [%]
1	None	78 (73) ^c
2	[Ir(dFCF ₃ ppy) ₂ dtbpy]PF ₆ as PC	62
3	4CzIPN as PC	64
4	<i>fac</i> -Ir(ppy) ₃ as PC	55
5	DCM instead of MeCN	47
6	Acetone instead of MeCN	51
7	DMF instead of MeCN	0
8	2.0 mL MeCN instead of 10.0 mL MeCN	60
9	0.2 equiv. TBAI instead of 2.0 equiv. TBAI	50
10	KI instead of TBAI	53
11	TBAB instead of TBAI	58
12	Disulfide instead of thiol	0
13	Without light	0
14	Without photocatalyst	0
15	Without TBAI	0

^a Reaction was carried out with **1a** (0.1 mmol), **2a** (2.0 equiv.), TBAI (2.0 equiv.), [Ir(dtbpy)ppy₂]PF₆ (3.0 mol%) in MeCN (10.0 mL) at ambient temperature using 30 W blue LED irradiation for 12 hours.

^b ¹H NMR yield using dimethyl terephthalate as an internal standard.

^c Isolated yield.

conditions. The results are presented in Table 1. After several initial experimental examinations, the optimal reaction conditions were identified as the following: ene-vinylidene cyclopropane (ene-VDCP) **1a** (0.2 mmol, 1.0 equiv.) was used as the substrate, 4-methylbenzenethiol **2a** (0.4 mmol, 2.0 equiv.) was employed as a reagent, TBAI (0.4 mmol, 2.0 equiv.) was used as an additive, and Ir[(dtbpy)ppy₂]PF₆ was utilized as a photosensitizer in acetonitrile (MeCN) (10.0 mL) under irradiation with a 30 W blue LED for 12 h, affording the desired product **3aa** in 78% NMR yield and 73% isolated yield (Table 1, entry 1). In addition, other photosensitizers such as Ir [(dFCF₃ppy)₂dtbpy]PF₆, 4CzIPN, and Ir(ppy)₃PF₆ afforded **3aa** in moderate yields of 55%–64% (entries 2–4) (see Tables S1–S7 in the ESI† for more information). We further examined solvent effects in this photochemical transformation and found that the use of other solvents, such as DCM, acetone and DMF, afforded **3aa** in lower yields ranging from 0% to 47%, demonstrating that the best solvent choice for the reaction was MeCN (entries 5–7) (see Table S2 in the ESI† for more information). When the solvent volume was changed to 2.0 mL, the yield of **3aa** decreased to 60% (entry 8) (see Table S6 in the ESI† for more information). In addition, when lowering the employed amount of TBAI to 0.2 equiv., the reaction efficiency decreased significantly (entry 9) (see Table S4 in the ESI† for more information). Moreover, we observed that other iodine anion sources or bromine anion sources gave **3aa** in lower yields (entries 10 and 11) (see Table S3 in the ESI† for more information). When using disulfide (Ph₂S₂) instead of thiol, no reaction occurred, indicating that disulfides or diselenides



Scheme 2 ^aStandard conditions: substrate 1 (0.1 mmol, 1.0 equiv.), 2 (2.0 equiv.), TBAI (2.0 equiv.), [Ir(dtbbpy)ppy₂]PF₆ (3.0 mol%) in MeCN (10.0 mL) at ambient temperature using 30 W blue LED irradiation for 12 hours. ^b No reaction. ^c The desired product was obtained in a complex mixture.

nides cannot be used instead of thiols or selenols (entry 12). Furthermore, the control experiments revealed that a photosensitizer, light, and TBAI were essential for this reaction (entries 13–15).

With the reaction conditions being optimized, we explored the generality of this cascade annulation reaction, and the results are summarized in Scheme 2. It was found that most of the substrates successfully underwent these reactions smoothly, providing the desired products in moderate to good yields. In order to investigate the electronic effect of the substituent R², the reactions were conducted using the substrates by altering the substituent R located at the *para* position on the benzene ring. The VDCPs **1b–1h** having either electron-withdrawing or -donating groups present on the benzene ring were all compatible in this reaction, and the desired products

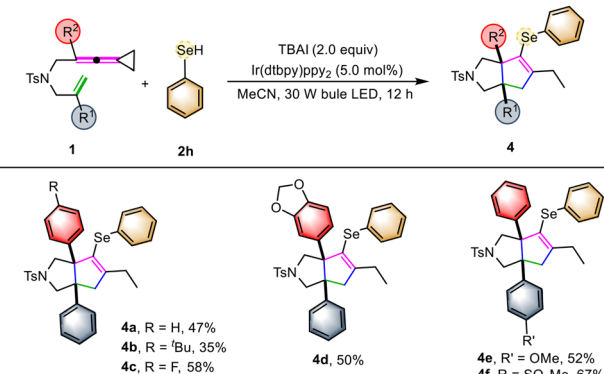
3ba–3ha were obtained in 57%–79% yields, revealing that the electronic property of R² had an impact on the yields of the product. When CF₃-substituted VDCP **1f** was utilized as the substrate, the desired product **3fa** was not produced in this reaction, probably due to the influence of its electronic effect. The structure of **3ga** was unambiguously determined by X-ray crystallographic analysis and its ORTEP drawing is shown in Scheme 2. In addition, its CIF data are summarized in the ESI.† When a *meta*-substituted methyl group was present at the benzene ring of VDCP **1i**, the corresponding product **3ia** was afforded in 61% yield. Product **3ja**, bearing a benzo[*d*][1,3]dioxole moiety, could be obtained in 60% yield under the standard conditions. Moreover, substrate **1k**, replacing the aryl group with a five-membered heterocyclic ring, could also afford the corresponding product **3ka** in 46% yield. However,

the reaction of a methyl-substituted substrate **1l** proceeded sluggishly, affording a complex mixture. As for VDCPs **1m** and **1n**, in which a cyclohexyl or a benzyl group was introduced, the corresponding products **3ma–3na** were produced in 53% and 43% yields, respectively. Next, we shifted our attention to examine the R¹ group in VDCPs **1** and found that introducing the substituents R' at the *ortho*-, *meta*-, and *para*-position on the benzene ring in VDCPs **1o–1s** gave the desired products **3oa–3sa** in moderate to good yields ranging from 61% to 87%, which is similar to those of R substituents. When a methyl group was present at R¹ in substrate **1t**, the corresponding product **3ta** was afforded in 41% yield. To our delight, upon changing the linker to an oxygen atom, the desired product **3ua** was obtained in 43% yield. Furthermore, when the (C(SO₂Ph)₂)-linked substrate **1v** was used to carry out the reaction, the desired product **3va** was furnished in 45% yield. Next, the R³ moiety of thiol reactants **2** was investigated. For the thiols containing a *para*-substituted benzene ring, the reactions took place smoothly, affording the target products **3ab–3ae** in 61–81% yields. However, when pentachlorothiophenol **2f** and alkyl-substituted thiol **2g** were used as the reactants, the reaction did not afford the desired products.

In order to further demonstrate the generality of this synthetic strategy, we then turned our attention to examining the substrate scope of **4** using selenol **2h** as the cyclization reactant (Scheme 3). Similarly, using VDCPs **1** as the substrates, the desired selenium-containing polycyclic products **4a–4f** were produced in moderate to good yields ranging from 35% to 67% under the standard conditions, indicating that this photochemical transformation is suitable for chalcogen-containing cyclic compounds. The substrates **1** having either electron-withdrawing or electron-donating groups present on the benzene ring were all tolerated in this reaction.

To gain more insights into the reaction mechanism, we carried out several control experiments (Scheme 4). First, the Stern–Volmer luminescence quenching analysis using TBAI and **2a** showed that both species can quench the emission of

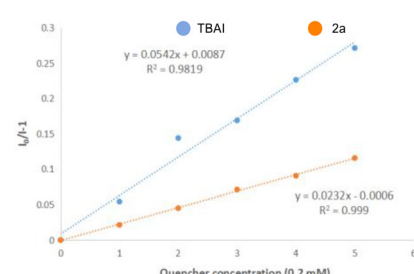
Ir[(dtbbpy)ppy₂]PF₆. However, the quenching efficiency of TBAI was much stronger than that of **2a** (Scheme 4A).¹⁰ The above result revealed that TBAI was an effective quencher for the excited state of Ir[(dtbbpy)ppy₂]PF₆. In order to investigate whether a free radical chaining process occurs in the reaction, we conducted the exclusive light-dependence of the reaction, in which the reaction basically stopped under dark conditions and continued when light was restored, indicating that visible light irradiation is a necessary condition for this reaction (Scheme 4B)¹¹ and the quantum yield was found to be $\phi = 0.005$ in this reaction (see S18 in the ESI†), also suggesting that the intervention of a radical chain mechanism is unlikely. In addition, when TEMPO was added to the reaction system as a radical scavenger, the reaction was inhibited completely, and the desired product **3aa** was not obtained (Scheme 4C). Subsequently, the reaction using deuterium-labeled thiophenol **d**₁-**2a** (90% D content) was conducted under the standard conditions, and we found that the deuterium atom was incorporated exclusively at the terminal carbon atom of **d**₁-**3aa**, showing that SET and HAT processes were both involved in the last step (Scheme 4D).¹² We also performed kinetic isotope experiments under the standard conditions (Scheme 4E). The parallel kinetic isotope effect was determined as $k_H/k_D = 2.02$ using **2a** and **d**₁-**2a** as the substrates; this result demonstrated that the initial HAT process might be involved in the rate-determining step following the rationale that C–D bond dissociation is harder than C–H bond dissociation.¹³ Furthermore, when acetic acid (2.0 equiv.) as a proton source was added to the reaction system in the presence of 0.2 equiv. of thiophenol **2a**, the intermediate **3aa'** was detected by LC-MS in 34% yield along with **3aa** in 12% yield (see Fig. S7 in the ESI† for more information). Then, we utilized **2e** as a nucleophilic reagent to react with intermediate **3aa'** in the presence of potassium carbonate, giving the desired product **3ea** in 53% yield. Therefore, we believed that the desired product **3aa** was obtained *via* intermediate **3aa'** through an intermolecular substitution reaction (Scheme 4F).¹⁴ We subsequently embarked on DFT calculations to gain insight into the reaction mechanism. All calculations were performed at the SMD(acetonitrile)/B3LYP/6-311+G(d,p)//B3LYP/6-31G(d) level using the Gaussian 16 program.¹⁵ The solvation Gibbs free energy profile in acetonitrile for the suggested reaction pathway is shown in Scheme 4G (see Table S8 in the ESI† for more information). We investigated the reaction pathway starting from the radical intermediate **INT1** shown in Scheme 4G. The intermediate **INT1** undergoes cyclization *via* **TS1** with an energy barrier of 15.0 kcal mol^{−1} to form an intermediate **INT2**, which produces the cyclized radical intermediate **INT3** through another intramolecular addition reaction with an energy barrier of 12.9 kcal mol^{−1}. We also investigated another possible cyclization process: cyclization of intermediate **INT1** *via* **TS1'** with an energy barrier of 26.8 kcal mol^{−1} forming an intermediate **INT2'** containing a five-membered ring (Scheme 4G); however, the energy barrier is relatively high and the transition state **TS2'** could not be located theoretically. Therefore, we excluded the pathway from **INT1** to **INT3** *via*



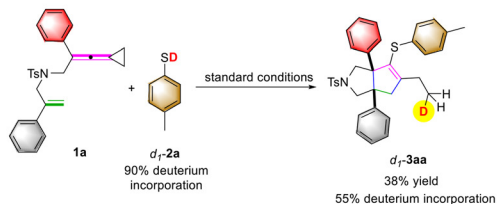
Scheme 3 Standard conditions: substrate **1** (0.1 mmol, 1.0 equiv.), **2h** (2.0 equiv.), TBAI (2.0 equiv.), [Ir(dtbbpy)ppy₂]PF₆ (3.0 mol%) in MeCN (10.0 mL) at ambient temperature using 30 W blue LED irradiation for 12 hours.



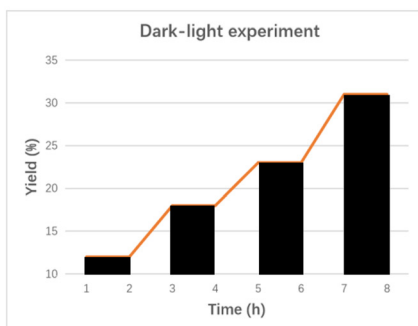
(A) Luminescence quenching experiments (Stern-Volmer Studies)



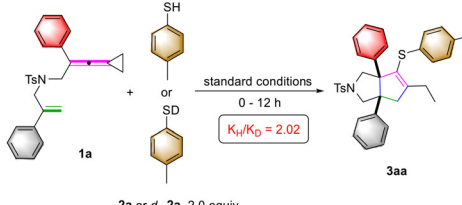
(D) Deuterium labeling experiments.



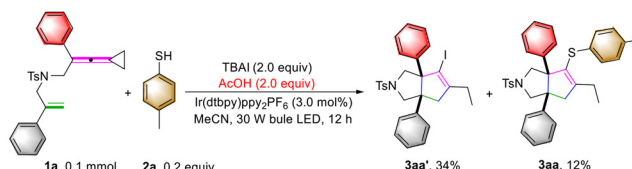
(B) Light on/off experiment.



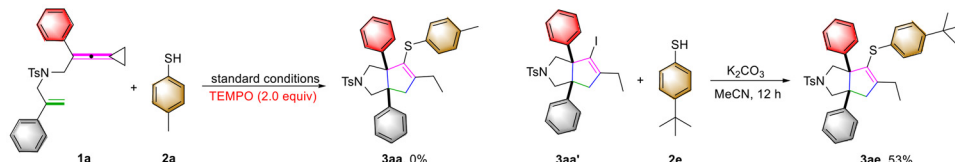
(E) Kinetic isotope effect experiment.



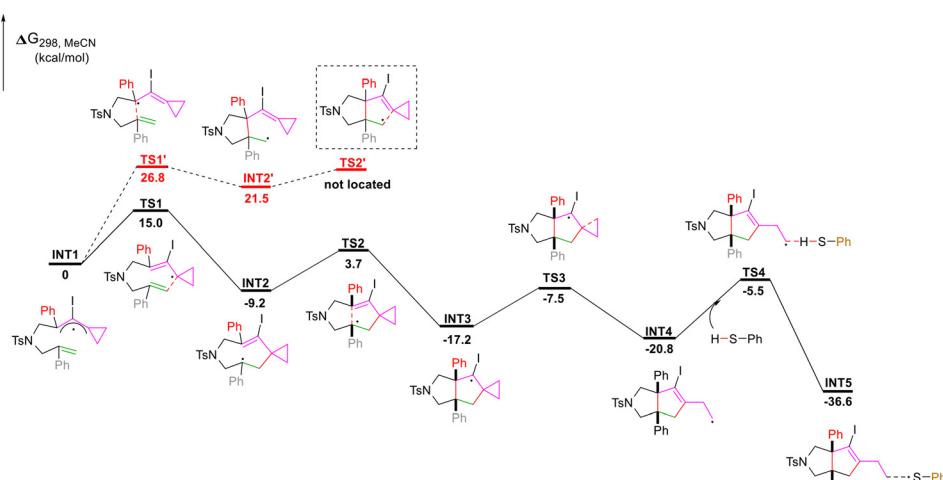
(F) Control experiment.



(C) Radical trapping experiments.



(G) DFT calculations

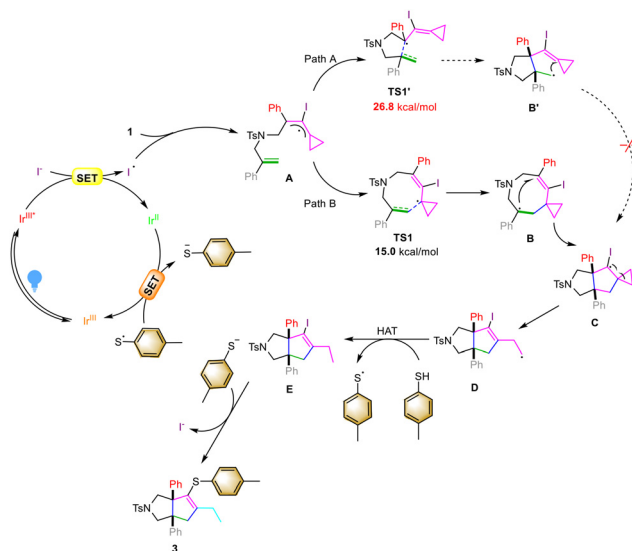


Scheme 4 Mechanistic studies. (A) Luminescence quenching experiments (Stern–Volmer Studies). (B) Light on/off experiment. (C) Radical trapping experiments. (D) Deuterium labeling experiments. (E) Kinetic isotope effect experiment. (F) Control experiment. (G) DFT calculation.

INT2'. The intermediate **INT3** undergoes a cyclopropane ring-opening process to give the radical intermediate **INT4** with an energy barrier of 9.7 kcal mol⁻¹. Subsequently, the intermediate **INT4** undergoes a HAT process with thiol **2a** to deliver the

intermediate **INT5** and a sulfur radical with an energy barrier of 15.3 kcal mol⁻¹. Based on the DFT calculations, the HAT process is the rate-determining step which agrees with the KIE result shown in Scheme 4E.



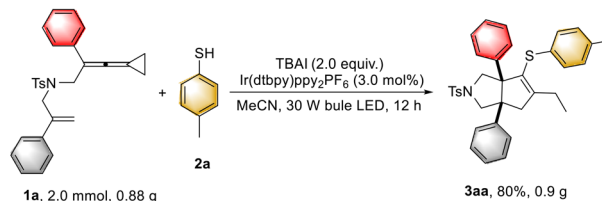
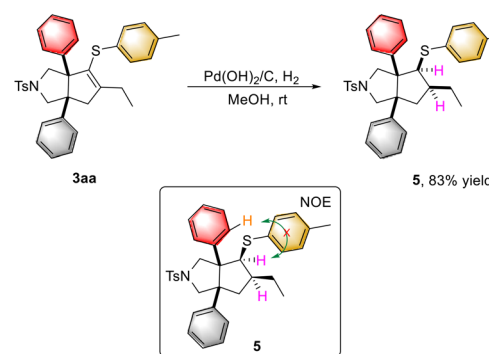
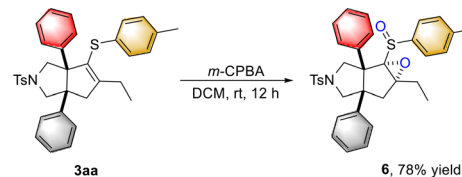
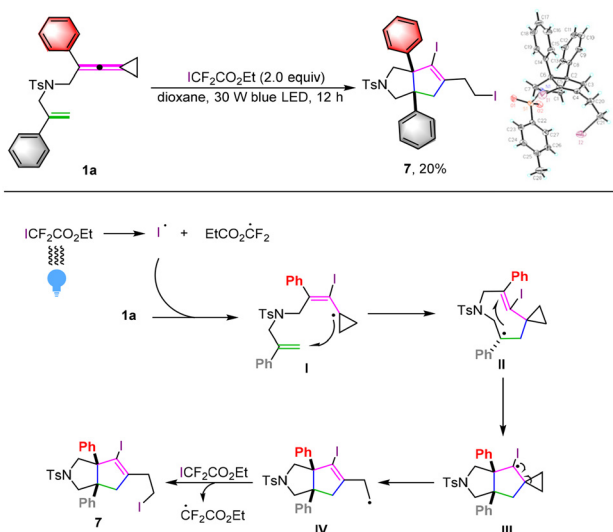


Scheme 5 The proposed reaction mechanism.

On the basis of control experiments and DFT calculations, we proposed a plausible mechanism to elucidate this visible light-induced photochemical reaction (Scheme 5). Upon irradiation with blue light, the ground state of the photosensitizer $\text{Ir}^{[\text{dtbbpy}]}\text{ppy}_2\text{PF}_6$ is converted into its excited state, which can further oxidize I^- through the SET process to afford the iodine radical, which tends to react with the allenyl moiety of VDCP **1** to furnish an iodinated radical intermediate **A**. The intermediate **A** undergoes cyclization *via* **TS1** with an energy barrier of $15.0 \text{ kcal mol}^{-1}$ to form an intermediate **B**, which produces a cyclized radical intermediate **C** through another intramolecular addition reaction. Based on the calculation results, cyclization of intermediate **A** *via* **TS1'** with an energy barrier of $26.8 \text{ kcal mol}^{-1}$ forms the intermediate **B'**. Thus, we exclude Path A from **A** to **C** *via* **B'**. The intermediate **C** undergoes a cyclopropane ring-opening process to furnish the radical intermediate **D**, which subsequently undergoes a HAT process with thiol **2a**¹³ to deliver intermediate **E** and a sulfur radical. Then, the *in situ* generated $\text{Ir}^{[\text{II}]}$ species reduces the sulfur radical to the corresponding sulfur anion, which can substitute the iodine atom in intermediate **E** to give the desired product **3** and close the catalytic cycle.¹⁴

To demonstrate the synthetic applicability of this protocol, a gram-scale reaction was conducted by using 0.88 g (2.0 mmol) of **1a**, obtaining the desired product **3aa** in 80% yield (0.9 g) under the standard conditions (Scheme 6A). Hydrogenation of the obtained product **3aa** effectively afforded the corresponding product **5** in 83% yield (Scheme 6B). Moreover, epoxidation of **3aa** with *m*-CPBA as an oxidant furnished the product **6** in 78% yield (Scheme 6C).

On the other hand, when we utilized ethyl iododifluoroacetate as the iodine source for the reaction, a new iodocyclization product **7** was obtained in 20% yield upon direct visible light irradiation (Scheme 7). Its structure has been unequivocally

A. Gram-scale reaction**B. Hydrogenative reduction reaction****C. Epoxidation reaction**Scheme 6 Synthetic transformations. (A) **1a** (2.0 mmol, 1.0 equiv.), **2a** (2.0 equiv.), TBAI (2.0 equiv.), $[\text{Ir}^{[\text{dtbbpy}]}\text{ppy}_2]\text{PF}_6$ (3.0 mol%) in MeCN (60.0 mL) at ambient temperature using 30 W blue LED irradiation for 12 hours; (B) $\text{Pd}(\text{OH})_2/\text{C}$, H_2 , MeOH, rt; (C) *m*-CPBA (2.5 equiv.).Scheme 7 **1a** (0.1 mmol, 1.0 equiv.), $\text{ICF}_2\text{CO}_2\text{Et}$ (2.0 equiv.), $\text{Ir}(\text{ppy})_3$ (5.0 mol%) in dioxane (10.0 mL) at ambient temperature using 30 W blue LED irradiation for 12 hours.

identified by X-ray diffraction and the ORTEP drawing is depicted in Scheme 7. A plausible reaction mechanism is also shown in Scheme 7. Upon direct irradiation with blue light, the iodine radical is generated from homolytic cleavage of ethyl iododifluoroacetate, which tends to react with **1a** to furnish an iodinated radical intermediate **I**. Subsequently, similar intramolecular cascade cyclization and cyclopropane ring-opening take place to afford radical intermediate **IV** through radical intermediates **II** and **III**, which reacts with ethyl iododifluoroacetate again to afford product **7** through a radical chain process.^{9e} In our previous paper, we have described that some unknown side reaction products could be formed upon photoirradiation of ethyl iododifluoroacetate.¹⁶

Conclusions

In summary, we have developed a novel and practical photo-redox catalytic methodology for iodine radical mediated cascade carbocyclization of ene-vinylidene cyclopropanes with thiols and selenols, delivering the chalcogen-containing polycyclic derivatives in moderate to good yields with broad substrate scope and good functional group tolerance under mild conditions. Moreover, this reaction could be achieved on a gram scale, and the products could be further functionalized to afford other novel polycyclic compounds. The reaction mechanism paradigm has been proposed on the basis of control experiments, deuterium labeling and photophysical analysis as well as DFT calculations. Further exploration of this visible light photoinduced synthetic strategy for the synthesis of medicinally useful products is underway.

Data availability

Experimental and computational data have been made available in the ESI.†

Author contributions

Z. Meng contributed to the investigation. Z. Meng, Y. Wei and M. Shi contributed to conceptualization and writing the original draft.

Conflicts of interest

There are no conflicts to declare.

Acknowledgements

We are grateful for the financial support from the National Key R & D Program of China (2022YFC2303100), the National Natural Science Foundation of China (21372250, 21121062,

21302203, 21772037, 21772226, 21861132014, 91956115 and 22171078) and the Fundamental Research Funds for the Central Universities 222201717003.

References

- (a) R. A. Bragg, S. Brocklehurst, F. Gustafsson, J. Goodman, K. Hickling, P. A. MacPaul, S. Swallow and J. Tugwood, Aortic Binding of AZD5248: Mechanistic Insight and Reactivity Assays To Support Lead Optimization, *Chem. Res. Toxicol.*, 2015, **10**, 1991–1999; (b) N. Z. Wang, P. Saidhareddy and X. F. Jiang, Construction of sulfur-containing moieties in the total synthesis of natural products, *Nat. Prod. Rep.*, 2020, **37**, 246–275; (c) R. Takeuchi, J. Shimokawa and T. Fukuyama, Development of a route to chiral epidithiodioxopiperazine moieties and application to the asymmetric synthesis of (+)-hyalodendrin, *Chem. Sci.*, 2014, **5**, 2003–2006; (d) T. C. Adams, J. N. Payette, J. H. Cheah and M. Movassaghi, Concise Total Synthesis of (+)-Luteoalbusins A and B, *Org. Lett.*, 2015, **17**, 4268–4271; (e) K. L. Rinehart, T. G. Holt, N. L. Fregeau, J. G. Stroh, P. A. Keifer, F. Sun, L. H. Li and D. G. Martin, Ecteinascidins 729, 743, 745, 759A, 759B, and 770: potent antitumor agents from the Caribbean tunicate Ecteinascidia turbinata, *J. Org. Chem.*, 1990, **55**, 4512–4515; (f) B. R. Beno, K. S. Yeung, M. D. Bartberger, L. D. Pennington and N. A. Meanwell, A Survey of the Role of Noncovalent Sulfur Interactions in Drug Design, *J. Med. Chem.*, 2015, **58**, 4383–4438.
- J. E. DeLorbe, D. Horne, R. Jove, S. M. Mennen, S. Nam, F. L. Zhang and L. E. Overman, General Approach for Preparing Epidithiodioxopiperazines from Trioxopiperazine Precursors: Enantioselective Total Syntheses of (+)- and (-)-Glioclidine C, (+)-Leptosin D, (+)-T988C, (+)-Bionectin A, and (+)-Gliocladin A, *J. Am. Chem. Soc.*, 2013, **135**, 4117–4128.
- (a) W. Hou and H. T. Xu, Incorporating Selenium into Heterocycles and Natural Products-From Chemical Properties to Pharmacological Activities, *J. Med. Chem.*, 2022, **65**, 4436–4456; (b) Y. Ogra, K. Ishiwata, H. Takayama, N. Aimi and K. T. Suzuki, Identification of a novel selenium metabolite Se-methyl-N-acetyl selenohexosamine, in rat urine by high-performance liquid chromatography-inductively coupled plasma mass spectrometry and -electrospray ionization tandem mass spectrometry, *J. Chromatogr. B: Anal. Technol. Biomed. Life Sci.*, 2002, **767**, 301–312; (c) P. Arsenyan, E. Paegle, I. Domracheva, A. Gulbe, I. K. Lapsa and I. Shestakova, Selenium analogues of raloxifene as promising antiproliferative agents in treatment of breast cancer, *Eur. J. Med. Chem.*, 2014, **87**, 471–483; (d) A. A. Vieira, I. R. Brando, W. O. Valenca, C. A. D. Simone, B. C. Cavalcanti, C. Pessoa, T. R. Carneiro, A. L. Braga and E. N. D. S. Júnior, Hybrid compounds with two redox centres: Modular synthesis of chalcogen-contain-



ing lapachones and studies on their antitumor activity, *Eur. J. Med. Chem.*, 2015, **101**, 254–265.

4 (a) R. P. Spencer, G. Montana, G. T. Scanlon and O. R. Evans, Uptake of selenomethionine by mouse and in human lymphomas, with observations on selenite and selenate, *J. Nucl. Med.*, 1967, **8**, 197–208; (b) J. Esteban, D. Lasa and S. P. Modrego, Detection of Cartilaginous Tumors with Selenium 75, *Radiology*, 1965, **85**, 149–150; (c) R. R. Cavalieri and K. G. Scott, Sodium Selenite Se 75: A More Specific Agent for Scanning Tumors, *J. Am. Med. Assoc.*, 1968, **206**, 591–595; (d) R. R. Cavalieri, K. G. Scott and E. Sairenji, Selenite (75Se) as a tumor-localizing agent in man, *J. Nucl. Med.*, 1966, **7**, 197–208.

5 (a) C. X. Li, R. J. Liu, K. Yin, L. R. Wen and M. Li, Synthesis of disulfides tethered pyrroles from β -ketothioamides via a bicyclization/ring-opening/oxidative coupling reaction, *Org. Biomol. Chem.*, 2017, **15**, 5820–5823; (b) Y. A. Zhang, Z. Ding, P. Liu, W. S. Guo, L. R. Wen and M. Li, Access to SCN-containing thiazolines via electrochemical regioselective thiocyanothiocyclization of N-allylthioamides, *Org. Chem. Front.*, 2020, **7**, 1321–1326; (c) B. B. Liu, H. W. Bai, H. Liu, S. Y. Wang and S. J. Ji, Cascade Trisulfur Radical Anion ($S_3^{\cdot-}$) Addition/Electron Detosylation Process for the Synthesis of 1,2,3-Thiadiazoles and Isothiazoles, *J. Org. Chem.*, 2018, **17**, 10281–10288.

6 (a) M. Randić, Aromaticity of Polycyclic Conjugated Hydrocarbons, *Chem. Rev.*, 2003, **103**, 3449–3606; (b) T. Nakata, Total Synthesis of Marine Polycyclic Ethers, *Chem. Rev.*, 2005, **105**, 4314–4347; (c) R. A. Craig and B. M. Stoltz, Polycyclic Furanobutenolide-Derived Cembranoid and Norcembranoid Natural Products: Biosynthetic Connections and Synthetic Efforts, *Chem. Rev.*, 2017, **117**, 7878–7909; (d) M. Hirai, N. Tanaka, M. Sakai and S. Yamaguchi, Structurally Constrained Boron-, Nitrogen-, Silicon-, and Phosphorus-Centered Polycyclic π -Conjugated Systems, *Chem. Rev.*, 2019, **119**, 8291–8331.

7 (a) K. G. Ji, H. T. Zhu, F. Yang, X. Z. Shu, S. C. Zhao, X. Y. Liu, A. Shaukat and Y. M. Liang, A Novel Iodine-Promoted Tandem Cyclization: An Efficient Synthesis of Substituted 3,4-Diiodoheterocyclic Compounds, *Chem. – Eur. J.*, 2010, **16**, 6151–6154; (b) C. Wan, J. Zhang, S. Wang, J. Fan and Z. Wang, Facile Synthesis of Polysubstituted Oxazoles via A Copper-Catalyzed Tandem Oxidative Cyclization, *Org. Lett.*, 2010, **12**, 2338–2341; (c) H. Batchu, S. Bhattacharya and S. Batra, Iodine-Mediated Intramolecular Electrophilic Aromatic Cyclization in Allylamines: A General Route to Synthesis of Quinolines, Pyrazolo[4,3-*b*]pyridines, and Thieno[3,2-*b*]pyridines, *Org. Lett.*, 2012, **14**, 6330–6333; (d) J. Zhang, Z. Wang, Y. Wang, C. Wan, X. Zheng and Z. Wang, A metal-free catalytic system for the oxidation of benzylic methylenes and primary amines under solvent-free conditions, *Green Chem.*, 2009, **11**, 1973–1978; (e) Q. Z. Li, L. Z. Yu, Y. Wei and M. Shi, Synthesis of Diiodinated All-Carbon 3,3'-Diphenyl-1,1'-spirobiindene Derivatives via Cascade Enyne Cyclization and Electrophilic Aromatic Substitution, *J. Org. Chem.*, 2019, **84**, 9282–9296; (f) J. Tang, C. Q. Zhao, S. Li, J. Zhang, X. L. Zheng, M. L. Yuan and H. Y. Fu, Tandem Ring-Contraction/Regioselective C-H Iodination Reaction of Pyridinium Salts, *J. Org. Chem.*, 2023, **88**, 2809–2821; (g) T. Khan and S. Yaragorla, Iodocyclization of Propargyl Alcohols: Highly Facile Approach to Hetero/Carbocyclic Iodides, *Eur. J. Org. Chem.*, 2019, **25**, 3989–4012; (h) U. P. N. Tran, G. Oss, M. Breugst, E. Detmar, D. P. Pace, K. Liyanto and T. V. Nguyen, Carbonyl-Olefin Metathesis Catalyzed by Molecular Iodine, *ACS Catal.*, 2019, **9**, 912–919; (i) M. Breugst, E. Detmar and D. von der Heiden, Origin of the Catalytic Effects of Molecular Iodine: A Computational Analysis, *ACS Catal.*, 2016, **6**, 3203–3212; (j) Y. F. Qiu, Y. J. Niu, X. R. Song, X. Wei, H. Chen, S. X. Li, X. C. Wang, C. D. Huo, Z. J. Quan and Y. M. Liang, Iodine promoted cascade cycloisomerization of 1-en-6,11-diyynes, *Chem. Commun.*, 2020, **56**, 1421; (k) Z. Meng, J. Yan, C. Ning, M. Shi and Y. Wei, Construction of pyrroles, furans and thiophenes via intramolecular cascade desulfonylative/dehydrogenative cyclization of vinylidene cyclopropanes induced by NXS (X = I or Br), *Chem. Sci.*, 2023, **14**, 7648–7655.

8 (a) S. Maejima, E. Yamaguchi and A. Itoh, trans-Diastereoselective Syntheses of γ -Lactones by Visible Light-Iodine-Mediated Carboesterification of Alkenes, *ACS Omega*, 2019, **3**, 4856–4870; (b) K. S. Kanyiva, T. Marina, S. Nishibe and T. Shibata, Metal-Free Aminiodination of Alkynes Under Visible Light Irradiation for the Construction of a Nitrogen-Containing Eight-Membered Ring System, *Adv. Synth. Catal.*, 2021, **363**, 2746–2751; (c) Y. K. Li, D. E. Wise, J. K. Mitchell and M. Parasram, Cascade Synthesis of Phenanthrenes under Photoirradiation, *J. Org. Chem.*, 2023, **88**, 717–721; (d) H. Liu, X. Fan, J. K. Hu, T. T. Ma, F. Wang, J. H. Yang and D. J. Li, Visible-Light-Enabled $\text{Ph}_3\text{P}/\text{LiI}$ -Promoted Tandem Radical Trifluoromethylation/Cyclization/Iodination of 1,6-Enynes with Togni's Reagent, *J. Org. Chem.*, 2022, **87**, 12877–12889; (e) Y. L. Lu, C. M. Chen, H. C. Zhu, Z. W. Luo and Y. H. Zhang, Highly efficient and fast synthesis of di-iodinated succinimide derivatives from 1,6-eyne and I_2 under air at room temperature, *Green Chem.*, 2022, **24**, 8021–8028; (f) Q. Cheng, F. R. Zhang, X. Y. Chen, Y. Han, C. G. Yan, Y. C. Shi, H. Hou and S. Q. Zhu, Visible-Light-Mediated Three-Component Radical Iodosulfonylative Cyclization of Enynes, *Org. Lett.*, 2022, **24**, 2515–2519; (g) M. Takeda, S. Maejima, E. Yamaguchi and A. Itoh, Direct lactonization from 1,3-dienes and malonate esters mediated by a combination of iodine and visible light, *Tetrahedron Lett.*, 2019, **60**, 151284; (h) S. Maejima, E. Yamaguchi and A. Itoh, Three-Component Iminolactonization Reaction via Bifunctionalization of Olefins Using Molecular Iodine and Visible Light, *J. Org. Chem.*, 2020, **85**, 10709–10718; (i) S. Maejima, E. Yamaguchi and A. Itoh, Intermolecular Tandem Addition/Esterification Reaction of Alkenes with



Malonates Leading to γ -Lactones Mediated by Molecular Iodine under Visible Light Irradiation, *Adv. Synth. Catal.*, 2017, **359**, 3883–3887; (j) A. Maity, B. L. Frey and D. C. Powers, Iodanyl Radical Catalysis, *Acc. Chem. Res.*, 2023, **14**, 2026–2036; (k) S. M. Hyun, M. B. Yuan, A. Maity, O. Gutierrez and D. C. Powers, The Role of Iodanyl Radicals as Critical Chain Carriers in Aerobic Hypervalent Iodine Chemistry, *Chem.*, 2019, **5**, 2388–2404; (l) C. P. Dong, K. Nakamura, T. Taniguchi, S. Mita, S. Kodama, S. Kawaguchi, A. Nomoto, A. Ogawa and T. Mizuno, Synthesis of Aryl Iodides from Arylhydrazines and Iodine, *ACS Omega*, 2018, **8**, 9814–9821; (m) S. Maejima, E. Yamaguchi and A. Itoh, Visible Light/Molecular-Iodine-Mediated Intermolecular Spirolactonization Reaction of Olefins with Cyclic Ketones, *J. Org. Chem.*, 2019, **15**, 9519–9531; (n) Y. Sudo, E. Yamaguchi and A. Itoh, Photo-oxidative Cross-Dehydrogenative Coupling-Type Reaction of Thiophenes with α -Position of Carbonyls Using a Catalytic Amount of Molecular Iodine, *Org. Lett.*, 2017, **7**, 1610–1613; (o) K. Oe, M. Goto, S. Maejima, E. Yamaguchi and A. Itoh, Front Cover: Cyanomethylation of β -Alkoxyaldehydes: Toward a Short Synthesis of Atorvastatin, *Asian J. Org. Chem.*, 2020, **9**, 1–5; (p) K. Usami, Y. Nagasawa, E. Yamaguchi, N. Tada and A. Itoh, Intermolecular Cyclopropanation of Styrenes Using Iodine and Visible Light via Carbon-Iodine Bond Cleavage, *Org. Lett.*, 2016, **1**, 8–11.

9 (a) M. Shi, L. X. Shao, J. M. Lu, Y. Wei, K. Mizuno and H. Maeda, Chemistry of Vinylidenecyclopropanes, *Chem. Rev.*, 2010, **110**, 5883–5913; (b) S. Yang and M. Shi, Recent Advances in Transition-Metal-Catalyzed/Mediated Transformations of Vinylidenecyclopropanes, *Acc. Chem. Res.*, 2018, **51**, 1667–1680; (c) D. H. Zhang, X. Y. Tang and M. Shi, Gold-Catalyzed Tandem Reactions of Methylenecyclopropanes and Vinylidenecyclopropanes, *Acc. Chem. Res.*, 2014, **47**, 913–924; (d) K. H. Rui and M. Shi, Rh(i)-Catalyzed intramolecular [3 + 2] cycloaddition reactions of yne-vinylidenecyclopropanes, *Org. Chem. Front.*, 2019, **6**, 1816–1820; (e) Z. Meng, X. Y. Zhang and M. Shi, Visible-light mediated cascade cyclization of ene-vinylidenecyclopropanes: access to fluorinated heterocyclic compounds, *Org. Chem. Front.*, 2021, **8**, 3796–3801; (f) C. Xu, C. Ning, S. Yang, Y. Wei and M. Shi, Rhodium-Catalyzed Asymmetric Cycloisomerization of 1,3-Diketones with Keto-Vinylidenecyclopropanes: Synthesis of Enantiomerically Enriched Cyclic β -Amino Alcohols, *Adv. Synth. Catal.*, 2021, **363**, 1727–1732; (g) C. Ning, K. H. Rui, Y. Wei and M. Shi, Rh(i)-catalyzed dimerization of ene-vinylidenecyclopropanes for the construction of spiro[4,5]decanes and mechanistic studies, *Chem. Sci.*, 2022, **13**, 7310–7317.

10 X. Y. Zhang, X. Y. Wu, B. Zhang, Y. Wei and M. Shi, Silyl Radical-Mediated Carbocyclization of Acrylamide-/Vinyl Sulfonamide-Attached Alkylidenecyclopropanes via Photoredox Catalysis with a Catalytic Amount of Silane Reagent, *ACS Catal.*, 2021, **11**, 4372–4380.

11 Y. Luo, Q. Wei, L. K. Yang, Y. Q. Zhou, W. D. Cao, Z. S. Su, X. H. Liu and X. M. Feng, Enantioselective Radical Hydroacylation of α,β -Unsaturated Carbonyl Compounds with Aldehydes by Triplet Excited Anthraquinone, *ACS Catal.*, 2022, **12**, 12984–12992.

12 (a) Q. Z. Li, X. T. Gu, Y. Wei and M. Shi, Visible-light-induced indole synthesis via intramolecular C–N bond formation: desulfonylative C(sp₂)-H functionalization, *Chem. Sci.*, 2022, **13**, 11623–11632; (b) S. Z. Nie, A. r Lu, E. L. Kuker and V. M. Dong, Enantioselective Hydrothiolation: Diverging Cyclopropenes through Ligand Control, *J. Am. Chem. Soc.*, 2021, **16**, 6176–6184.

13 (a) J. M. Mayer, Understanding Hydrogen Atom Transfer: From Bond Strengths to Marcus Theory, *Acc. Chem. Res.*, 2011, **44**, 36–46; (b) W. G. Zhang, Z. L. Zou, Y. H. Wang, Y. Wang, Y. Liang, Z. G. Wu, Y. X. Zheng and Y. Pan, Leaving Group Assisted Strategy for Photoinduced Fluoroalkylations Using N-Hydroxybenzimidoyl Chloride Esters, *Angew. Chem., Int. Ed.*, 2019, **58**, 624–627.

14 (a) Z. Rappoport and A. Topol, Nucleophilic attacks on carbon–carbon double bonds 26 Stereoconvergence in nucleophilic vinylic substitution of an activated nitro olefin, *J. Am. Chem. Soc.*, 1980, **102**, 406–407; (b) Z. Rappoport and A. Topol, Nucleophilic attacks on carbon–carbon double bonds. Part 39 Nucleophile and nucleofuge effects, catalysis and stereochemistry in vinylic substitution of electrophilic nitro olefins, *J. Org. Chem.*, 1989, **54**, 5967–5977.

15 M. J. Frisch, G. W. Trucks, H. B. Schlegel, G. E. Scuseria, M. A. Robb, J. R. Cheeseman, G. Scalmani, V. Barone, G. A. Petersson, H. Nakatsuji, X. Li, M. Caricato, A. V. Marenich, J. Bloino, B. G. Janesko, R. Gomperts, B. Mennucci, H. P. Hratchian, J. V. Ortiz, A. F. Izmaylov, J. L. Sonnenberg, D. Williams-Young, F. Ding, F. Lipparini, F. Egidi, J. Goings, B. Peng, A. Petrone, T. Henderson, D. Ranasinghe, V. G. Zakrzewski, J. Gao, N. Rega, G. Zheng, W. Liang, M. Hada, M. Ehara, K. Toyota, R. Fukuda, J. Hasegawa, M. Ishida, T. Nakajima, Y. Honda, O. Kitao, H. Nakai, T. Vreven, K. Throssell, J. A. Montgomery Jr., J. E. Peralta, F. Ogliaro, M. J. Bearpark, J. J. Heyd, E. N. Brothers, K. N. Kudin, V. N. Staroverov, T. A. Keith, R. Kobayashi, J. Normand, K. Raghavachari, A. P. Rendell, J. C. Burant, S. S. Iyengar, J. Tomasi, M. Cossi, J. M. Millam, M. Klene, C. Adamo, R. Cammi, J. W. Ochterski, R. L. Martin, K. Morokuma, O. Farkas, J. B. Foresman and D. J. Fox, *Gaussian 16, Revision A.03*, Gaussian, Inc., Wallingford CT, 2016.

16 Z. Liu, Y. Wei and M. Shi, Visible-light-mediated interrupted Cloke-Wilson rearrangement of cyclopropyl ketones to construct oxy-bridged macrocyclic framework, *Tetrahedron Org.*, 2022, **1**, 10001.

